

## Soft-x-ray magnetic circular dichroism on a paramagnetic two-iron system

J. van Elp\*

*Energy and Environment Division, Lawrence Berkeley Laboratory, Berkeley, California, 94720*

G. Peng

*Department of Applied Science, University of California, Davis, California 95616*

Z. H. Zhou, S. Mukund, and M. W. W. Adams

*Department of Biochemistry and Center for Metalloenzyme Studies, University of Georgia, Athens, Georgia 30602*

(Received 25 January 1995; revised manuscript received 1 August 1995)

The sign of the x-ray magnetic circular dichroism signal has in general been used to determine the magnetic coupling between ions with different oxidation states or different elements. We have investigated the coupling between two distorted-tetrahedral-coordinated irons with two different oxidation states in a dinuclear cluster. The two iron atoms are antiferromagnetically coupled and because of a strong chemical shift between the two oxidation states one would expect to see an up-down effect in the magnetic circular dichroism signal at the iron  $L_3$  edge. We observe an only positive effect, which is inconsistent with a strong antiferromagnetic coupling. We can explain the results by taking the individual zero-field splittings of both iron atoms into account. This study uses magnetic circular dichroism in the soft-x-ray range to study the magnetic coupling between transition-metal sites in paramagnetic clusters, and although still limited by low count rates it shows the potential and subtleties of this technique.

### INTRODUCTION

Magnetic x-ray dichroism measures differences in absorption between polarized x rays at inner-shell absorption edges. Strong magnetic dichroism effects in the soft-x-ray region were predicted by Thole, van der Laan, and Sawatzky<sup>1</sup> for the rare-earth  $M_{4,5}$  edges about a decade ago, after which a linear magnetic dichroism effect was experimentally observed at the terbium  $M_5$  edge.<sup>2</sup> In the hard-x-ray region a small magnetic circular dichroism effect was observed at the iron  $K$  edge.<sup>3</sup> Since the initial experiments, attention has partly been focused on using x-ray magnetic circular dichroism (XMCD) to study magnetic ordering. The sign of the magnetic coupling between magnetic sublattices or between an impurity and a host can be studied because a ferromagnetic coupling is visible as two positive XMCD signals for the different oxidation states, or absorption edges, and an antiferromagnetic coupling as a positive and a negative XMCD signal. In gadolinium iron garnet<sup>4</sup> the element-specific Fe and Gd XMCD showed that the local magnetic moments are reversed upon crossing the compensation point. The interaction of metal impurities with their metal hosts has also been studied using the sign and magnitude of impurity  $L_{2,3}$  edges XMCD.<sup>5,6</sup> The study of magnetic moments by XMCD received a strong impetus through the recently derived magneto-optical sum rules,<sup>7,8</sup> which link measured XMCD intensities to the local spin and orbital moments in the ground state.

Recently, we reported soft XMCD results on a dilute paramagnetic system.<sup>9</sup> A strong effect was observed at the Fe  $L_{2,3}$  edges of a high-spin iron site in a metalloprotein. For paramagnetic systems, orientation of the paramagnetic moment requires strong magnetic fields and low temperatures. Ferromagnetic or antiferromagnetic coupling is not limited to bulk

magnetic systems but can also be found in metal-containing clusters in inorganic compounds and metalloproteins. We have investigated and obtained results on an antiferromagnetically coupled paramagnetic system with two iron atoms in the cluster. In the reduced form this paramagnetic  $S=1/2$  cluster contains antiferromagnetically coupled localized  $\text{Fe}^{2+}$  and  $\text{Fe}^{3+}$  ions, with a clear chemical shift between the two oxidation states. Magnetic susceptibility measurements<sup>10,11</sup> on clusters with similar coordination showed that in the reduced form they are antiferromagnetically coupled with an exchange parameter  $J$  of about  $-100 \text{ cm}^{-1}$ . Because of the antiferromagnetic coupling one expects to see a negative and a positive effect at the iron  $L_3$  edge upon orientation of the total spin, even if we take the spin coupling of an atomic  $\text{Fe}^{2+}, \text{Fe}^{3+}$  coupled system to an  $S=1/2$  total spin into account. However, we observed only a positive XMCD effect, localized at the  $\text{Fe}^{3+} L_3$  edge position. A possible explanation is suggested based on a modeling of the local ligand fields and takes into account the individual zero-field-splitting (ZFS) patterns of the two iron atoms.

### EXPERIMENTAL SECTION

The experiments were performed using the AT&T bending magnet beamline U4B (Ref. 12) at the National Synchrotron Light Source, Brookhaven National Laboratory. We obtained a degree of circular polarization of around 80% by moving the vertical focusing mirror above or below the plane of the electron orbit. The energy resolution used was 225 meV in the absorption experiments (linear polarized light) and 650 meV for the circular polarized experiments. To orient the magnetic moment of the paramagnetic system we used a split-coil, cold-bore, and ultrahigh-vacuum-compatible superconducting magnet with a separate cryostat

for the sample.<sup>9</sup> A magnetic field of 6T was used and the sample cryostat was cooled down to 1.5 K. A thin aluminum window attached to the cryostat in front of the sample was used to shield the sample from infrared radiation, ensuring that the sample reached temperatures close to 1.5 K. Because of the dilute nature of the cluster of two iron ions the absorption spectra are detected using a 13-element germanium fluorescence detector,<sup>13</sup> positioned at the node of the magnetic field, in between the coils of the superconducting magnet. In the  $L_{2,3}$  edge absorption experiments the fluorescence detector was positioned as close as possible to the sample to optimize the count rate. The resolution of the detector is about 150 eV, which makes it possible to discriminate between oxygen signals at 525 eV and iron fluorescence signals at 710 eV.

The two-iron cluster in *C. pasteurianum* ferredoxin is a clear example of a dinuclear paramagnetic system with antiferromagnetic coupling.<sup>14</sup> It has a molecular weight of 23 kDa, and was purified at the University of Georgia, Athens by following published procedures.<sup>15</sup> Samples of the reduced and oxidized forms were prepared in an anaerobic glovebox as partially dehydrated thin films on a gold-coated copper sample holder, and were anaerobically transferred to the superconducting magnet or  $L$  edge experimental chamber.

Both the direction of the magnetic field and the circular polarization were interchanged in the XMCD measurements. Although the circular polarized absorption spectra shown are averages of different polarizations and magnetic-field directions, we will, for simplicity, refer to them as left and right circular polarized light. In each data set zero-magnetic-field scans were taken to calibrate the energy of the circular polarized photons. For the zero-field calibration scans the detector is positioned as close as possible to the sample, and spectra with good statistics are obtained. The relative energy calibration is done with great accuracy. We corrected for small energy offsets ( $\approx 50$  meV) in the data sets caused by slightly different light paths for left and right circular polarized light. The XMCD spectrum was obtained as the difference between the left and right circular polarized spectra. The left and right sum spectra are normalized to equal intensity in front of the  $L_3$  edge and at 10 eV beyond the  $L_2$  edge. The difference of the  $L$  edge spectra is obtained before a background is subtracted in the  $L$  edge spectra. The XMCD spectrum is sensitive to a correct energy calibration of the left and right circular light spectra, but not very sensitive to the intensity normalization. To enhance the  $2p$ -to- $3d$  spectral weight of the  $L_{2,3}$  absorption edges we show the  $L_{2,3}$  edge spectra after a background is subtracted using a fit to a polynomial function in front of the  $L_3$  edge and 10 eV beyond the  $L_2$  edge. The absolute energy scale was calibrated using  $K_4Fe(CN)_6$ , assuming  $L_3$  edge absorption peaks at 710.35 and 712.05 eV.

Because of the fluorescence photon detection technique, a possible error may be introduced in the XMCD spectrum because besides the XMCD effect in the absorption process we also have an unwanted XMCD effect in the fluorescence emission. Based on a recent high-resolution x-ray-emission MCD study on iron, cobalt, and nickel,<sup>16</sup> we estimate that these emission effects will change the XMCD intensity by 10% at most. The reason for this is twofold. Excited  $d^n$  states are possible as final states in the emission process, which

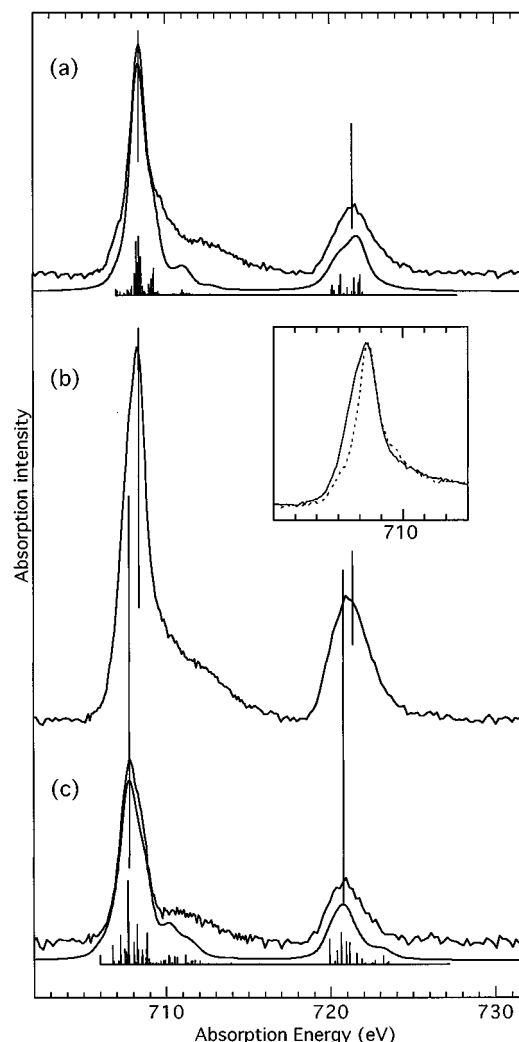


FIG. 1. Iron  $L_{2,3}$  edge absorption spectra of the two-iron cluster. (a) Experimental spectrum (top) of the oxidized form (two  $Fe^{3+}$  ions) together with a theoretical calculation (bottom). (b) Experimental spectrum of the reduced form (one  $Fe^{3+}$  and one  $Fe^{2+}$ ). (c) The  $Fe^{2+}$  component of the reduced form (top) together with a theoretical calculation (bottom). The vertical lines below the theoretical calculations show the strengths and positions of the individual transitions before line broadening. The inset in (b) compares the  $L_3$  edges of the reduced (solid line) and oxidized (dashed line) forms, when normalized to equal intensity at the  $L_3$  edge.

open up a larger number of decay channels. We also detect all  $L$  edge photons because of the large window of the detector, which means that we do detect processes in which, because of relaxation of the core hole, the polarization is lost and no emission dichroism can be observed. In the high-resolution x-ray-emission results on iron, cobalt, and nickel<sup>16</sup> this is clearly visible when the absorbing photon has the energy of the  $L_2$  edge, but most of the emission photons are observed at the  $L_3$  edge.

## RESULTS AND DISCUSSION

The changes at the iron  $L_{2,3}$  edges for both oxidation states are shown in Fig. 1. The oxidized form consists of two distorted-tetrahedral-symmetry  $Fe^{3+}$  sites, bridged by two la-

ble sulfurs. Also, each iron has two additional sulfur ligands from cysteine side chains. The reduced form has an  $\text{Fe}^{2+}$  and an  $\text{Fe}^{3+}$  site with similar coordination. The inset in Fig. 1 shows the strong difference at the  $L_3$  edge between the reduced and oxidized forms, when both spectra are normalized to the maximum of their  $L_3$  edge intensity. It is very clear that the reduction of one iron site introduces a shift of spectral weight to lower absorption energy. Figure 1(c) shows the spectrum of the  $\text{Fe}^{2+}$  component of the reduced form, which we obtained after subtracting the spectrum of the oxidized form with 55% of the total intensity. We assume in this subtraction that the total absorption intensity relates directly to the number of  $3d$  holes for both oxidation states, assuming (because of covalency) 6.3  $d$  electrons for a divalent iron and 5.5  $d$  electrons for a trivalent iron. Upon reduction we find a 600 meV shift for both  $L$  edges. A slightly larger shift (800 meV) has been observed in a similarly coordinated single-iron system.<sup>17</sup>

The calculations shown for the oxidized form ( $\text{Fe}^{3+}$ ) and for the  $\text{Fe}^{2+}$  component of the reduced form are atomic multiplet calculations with the inclusion of an adjustable ligand field.<sup>18</sup> They have been widely used for  $3d$  transition-metal compounds<sup>19,20</sup> and, recently, also for isolated metal centers.<sup>17,21</sup> The parameters obtained<sup>22</sup> show the near-tetrahedral symmetry at both iron sites with  $10Dq$  values of  $-0.5$  eV for the oxidized form and  $-0.6$  eV for the  $\text{Fe}^{2+}$  component of the reduced form. The Slater integrals were reduced to 50% and 65% as compared to the *ab initio* values,<sup>18</sup> consistent with a greater covalency for the  $\text{Fe}^{3+}$  site. Reducing the symmetry to  $D_{2d}$ , which splits up the  $e$  and  $t_2$   $3d$  orbitals, does not improve the  $L$  edge absorption calculation.

In Fig. 2 we show the left and right circular polarized spectra for the reduced form (the oxidized form has, of course, no XMCD effect). We observe a strong, but only positive, 12% XMCD effect [as defined by  $(I_r - I_l)/(I_r + I_l)$ ] at the  $L_3$  edge and a negative, but weak, XMCD effect at the  $L_2$  edge. At each edge the XMCD signal has only one sign. If we plot the dichroism signal on the same scale as the absorption edge signals as we have done in Fig. 3, it becomes very clear that the XMCD effect is limited to the  $\text{Fe}^{3+}$  component of the reduced spectrum, and that the  $\text{Fe}^{2+}$  component has within noise no XMCD effect.

Before we try to explain our results we will discuss the magnetic coupling between the two iron sites and the zero-field-splitting patterns of single-iron systems. Magnetic susceptibility measurements<sup>10,11</sup> show that in both forms we have an antiferromagnetic coupling with an exchange parameter  $J$  of about  $-200$   $\text{cm}^{-1}$  for the oxidized form and  $-100$   $\text{cm}^{-1}$  for the reduced form. The magnetic coupling in the two-iron cluster is different from the coupling between different sublattices in a solid. We will couple both iron spins antiferromagnetically to an  $S=1/2$  total spin, using spin vector addition. To obtain information about the XMCD effect in this coupled system, we have to know what the character of the  $m_s = -1/2$  part of the total spin  $S=1/2$  antiferromagnetically coupled level is, in terms of  $m_s$  values for the individual  $\text{Fe}^{2+}$  and  $\text{Fe}^{3+}$  sites. Remember that in this experiment, because of the chemical shift between the two oxidation states, we probe the individual magnetization or occupation of these  $m_s$  levels as compared to, for instance, electron

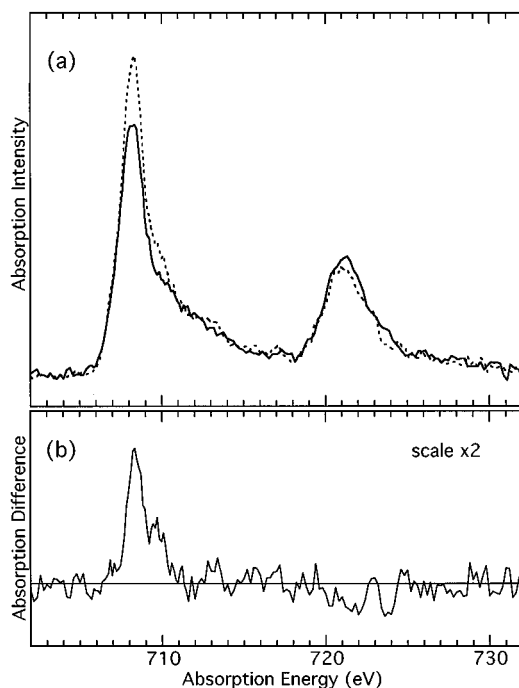


FIG. 2. (a) The right (dashed line) and the left (solid line) circular polarized absorption spectra from the two-iron cluster. (b) The soft-x-ray magnetic circular dichroism spectrum (right minus left circular polarized light), with the intensity multiplied by 2.

paramagnetic resonance (EPR) or magnetic susceptibility measurements.

The strength of the XMCD effect for each oxidation state is directly related to the occupation of the  $m_s$  levels or magnetization of the individual oxidation states. For a single divalent iron ion with  $S=2$ , the XMCD effect is strongest for  $m_s = -2$ , weaker for  $m_s = -1$ , with about half of the XMCD intensity, and zero for the nondegenerate  $m_s = 0$  level. In this last case the same final states are reached with left and right circular polarized light. A similar situation with respect to the strength of the XMCD signal exists for the trivalent iron.

Clebsch-Gordan or vector addition coefficients for coupling of an  $S=2$  spin are tabulated in Ref. 23, and we obtain for the  $m_s = -1/2$  level as written as a sum of  $\phi(m_1, m_2)$ ,

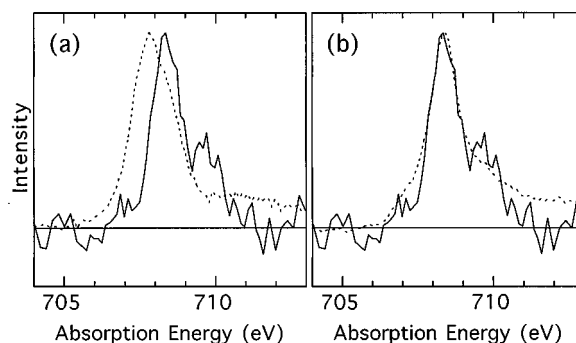


FIG. 3. Comparison of the observed XMCD signal (solid line) with the  $L_3$  edges of (a) the  $\text{Fe}^{2+}$  component of the reduced form, and (b) the oxidized ( $\text{Fe}^{3+}$ ) form of the two-iron cluster.

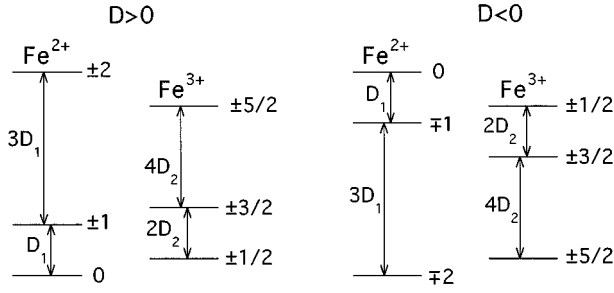


FIG. 4. Schematic diagram of the zero-field splittings for both iron sites with  $D > 0$  and  $D < 0$ . The size of the splittings ( $D_1$  and  $D_2$ ) is not to scale.

with  $m_1$  ( $m_2$ ) the  $m$  value of the  $S_1=2$  ( $S_2=5/2$ ) spin

$$\Psi(S=\frac{1}{2}, m_s=-\frac{1}{2}) = \sqrt{\frac{1}{15}}\phi(-2, \frac{3}{2}) - \sqrt{\frac{2}{15}}\phi(-1, \frac{1}{2}) \\ + \sqrt{\frac{3}{15}}\phi(0, -\frac{1}{2}) - \sqrt{\frac{4}{15}}\phi(1, -\frac{3}{2}) + \sqrt{\frac{5}{15}}\phi(2, -\frac{5}{2}).$$

Because of the large Clebsch-Gordan coefficient in front of the  $\phi(2, -5/2)$  component, we find upon full orientation of the  $S=1/2$  spin a main alignment of the moment of the  $S=5/2$  spin with the  $S=2$  spin coupled antiparallel. It is important to realize that neither of the two individual spins is fully oriented because we have an occupation of different individual  $m_s$  levels in the wave function, instead of the  $m_s=-5/2$  ( $+2$ ) for the  $S=5/2$  ( $2$ ) spin. The predicted XMCD effect at the  $L_3$  edge would be negative for the  $\text{Fe}^{2+}$  component and positive for the  $\text{Fe}^{3+}$  component, but smaller than would be observed for two fully oriented individual iron sites. In using spin vector addition we have assumed that the exchange coupling is the dominant interaction in the Hamiltonian describing the low-energy physics.

For single-iron systems the strength of the XMCD effect is determined by the interplay between the magnetization and the zero-field splittings (ZFS's). In the distorted-tetrahedral  $\text{Fe}^{3+}$  symmetry the ZFS is caused by spin-orbit coupling of the ground level with the low-lying excited states, which split up the  ${}^6A_1$  ( $T_d$  symmetry) ground level into three sublevels (see Fig. 4). The ZFS parameter  $D$  describes the size of the splitting and is positive for the fourfold-sulfur-coordinated  $\text{Fe}^{3+}$  site in low-molecular-weight proteins<sup>24</sup> as well as in the inorganic compound  $(\text{Et}_4\text{N})[\text{Fe}(\text{SR})_4]$  (Et indicates an ethyl and R an alkyl group), which has a very similar tetrahedral coordination.<sup>25</sup> In the absence of a magnetic field, we find a strongly mixed  $m_s=\pm 1/2$  level as the lowest sublevel with an  $m_s=\pm 3/2$  level at  $2D$  and an  $m_s=\pm 5/2$  level at  $6D$ , ignoring axial and rhombic terms. Because the ZFS parameter  $D$  is small ( $\approx 2 \text{ cm}^{-1}$ ) a strong magnetic field will mix these levels, adding to the lowest level a large amount of  $m_s=-5/2$ . This explains the strong dichroism observed in our soft-x-ray MCD experiments on a trivalent single-iron site in a metalloprotein.<sup>9</sup>

For an  $\text{Fe}^{2+}$  in distorted-tetrahedral symmetry the ZFS splits the ground state in first approximation into sublevels with mixed  $m_s=\pm 2$  character at  $4D$  and  $m_s=\pm 1$  character at  $D$  as compared to the nondegenerate  $m_s=0$  level. A

negative value of about  $-10 \text{ cm}^{-1}$  is reported in an optical MCD study of the inorganic system  $(\text{Et}_4\text{N})_2[\text{Fe}(\text{SR})_4]$ .<sup>26</sup> We also found because of a large XMCD effect an  $m_s=\pm 2$  as lowest level and  $D < 0$  for a divalent iron in a distorted-tetrahedral symmetry in a metalloprotein.<sup>27</sup>

So for the single distorted-tetrahedral iron we find for  $\text{Fe}^{3+}$  a positive ZFS parameter  $D$  and for  $\text{Fe}^{2+}$  a negative  $D$ . Using a  $D_{2d}$  distortion, a positive  $D$  for  $\text{Fe}^{3+}$  is obtained when the  $3d$  orbital splitting has  $d_{z^2}$  as the lowest unoccupied orbital. For  $\text{Fe}^{2+}$  we have a negative  $D$  which means that the lowest unoccupied orbital is  $d_{z^2}$  (the  $d_{x^2-y^2}$  is the only minority-spin-filled orbital). The sign of  $D$  (Refs. 25,26) is determined for both valencies by the sign of the splitting between the  $d_{x^2-y^2}$  and  $d_{z^2}$ , so for both a positive (negative)  $D$  has  $d_{z^2}$  ( $d_{z^2-y^2}$ ) as the lowest orbital.

We can formulate now two spin-coupled models (see Fig. 4) based on a modeling of the local ligand fields. The system can be described as two individual irons with two individual zero-field splittings, but the system is antiferromagnetically coupled. First, we have for both sites  $D < 0$ , so a mixed  $m_s=\pm 5/2$  for the trivalent  $S=5/2$  and the mixed  $m_s=\pm 2$  for the divalent  $S=2$ , coupled antiferromagnetically together to a total  $m_s=\pm 1/2$ . In this situation we expect to see large XMCD effects for both oxidation states and an up-down effect at the  $L_3$  edge upon full magnetization of the total  $S=1/2$  spin, because both iron sites will be fully magnetized, occupying  $m_s=-5/2$  and  $m_s=+2$ . As a second model we can have for both sites  $D > 0$ . In this case we have a mixed  $m_s=\pm 1/2$  level for the  $S=5/2$  and the nondegenerate  $m_s=0$  level for the  $S=2$ ; coupled together antiparallel we have again  $m_s=\pm 1/2$ . Now we expect to observe no XMCD effect at the  $\text{Fe}^{2+}$  site because we have a nondegenerate state and a small XMCD effect at the  $\text{Fe}^{3+}$  site because of the  $m_s=\pm 1/2$  level.

Clearly our result can be explained by assuming that  $D$  is positive for both sites, and that the exchange interaction is weak as compared to the individual ZFS pattern. At first sight the values for the different parameters do not indicate this. For similar two-iron clusters a value for the exchange interaction of about  $-100 \text{ cm}^{-1}$  is reported.<sup>10,11</sup> For  $\text{Fe}^{2+}$  in a distorted-tetrahedral symmetry an experimental value of  $D=-8.7 \text{ cm}^{-1}$  was obtained<sup>26</sup> for the inorganic model compound  $(\text{Et}_4\text{N})_2[\text{Fe}(\text{SR})_4]$ . Using ligand-field atomic multiplet calculations for  $\text{Fe}^{2+}$  in a  $D_{2d}$  symmetry with a reasonable value for the distortion of  $D_s=100 \text{ meV}$  ( $10Dq=-0.6 \text{ eV}$ ), we find a value of  $D$  around  $10 \text{ cm}^{-1}$ . The zero-field splitting for  $\text{Fe}^{3+}$  is found to be small ( $\approx 2 \text{ cm}^{-1}$ ) in the earlier-mentioned optical MCD experiment<sup>24</sup> and also in the  $D_{2d}$  calculation, using again a splitting  $D_s=100 \text{ meV}$ . So both ZFS parameters observed on and deduced for single-iron sites are about an order of magnitude smaller than the value of the exchange coupling. However, the absence of an XMCD effect at the  $\text{Fe}^{2+}$  position strongly suggests that the ZFS patterns are important, and our experimental result can be explained by a modeling of the local ligand fields for both iron sites.

For positive  $D$  we find the  $d_{z^2}$  orbital as the only occupied minority-spin orbital at the  $\text{Fe}^{2+}$  site. This was also observed in Mössbauer studies<sup>14,28</sup> on these reduced two-iron clusters. A large quadrupole splitting was found, and from this large splitting it was deduced that  $d_{z^2}$  is the occupied minority-

spin orbital, and that the site is highly covalent. A positive  $D$  for both sites means that the  $d_{z^2}$  orbital at the  $\text{Fe}^{3+}$  sites is the orbital which accepts at one of these sites the electron upon reduction.

### CONCLUDING REMARKS

In conclusion, both iron sites are well distinguishable because of a chemical shift between the two oxidation states. We observed only a positive  $L_3$  edge XMCD effect localized at the  $\text{Fe}^{3+}$  site, in an antiferromagnetically coupled paramagnetic two-iron system. Although one might expect the low-energy physics for this system to be determined by the value of the exchange coupling parameter  $J$ , the results can be explained using a simple model of two individual irons with their individual ZFS's. We find the sign of the zero-field splittings for both sites to be positive and the lowest orbital of  $d_{z^2}$  character, as also has been observed in a Mössbauer study.

Although our study is still limited by low count rates it shows the potential and subtleties of soft-x-ray magnetic circular dichroism for studying the individual magnetization of different oxidation states or different elements in paramagnetic clusters. This technique is different from EPR or sus-

ceptibility measurements in which the total spin is investigated. A full analysis of such systems in which one would like to obtain quantitative information about the ZFS pattern parameters  $D$  and the exchange interaction will require a detailed measurement of XMCD magnetization curves at different fields and temperatures. Such an analysis is outside the scope of the present work. It is clear, however, that we have observed an interesting effect, which is not expected assuming a strong exchange coupling between the two irons.

### ACKNOWLEDGMENTS

We have appreciated discussions with and help received from J. Christiansen, C. Ralston, S. J. George, S. P. Cramer, S. Mitra-Kirtley, P. Kuiper, E. Pellegrin, H.-J. Lin, and C. T. Chen. This research was supported by the National Science Foundation through Grant No. DMB-88-05-255 (to M.W.W.A.), and by Lawrence Berkeley Laboratory LDRD Exploratory Research Funds. The Center for Metalloenzyme Studies at the University of Georgia is funded by a grant from the National Science Foundation (DIR-9014281), and the National Synchrotron Light Source is supported by the Department of Energy, Office of Basic Energy Sciences.

- 
- \*Present address: ISA, Institute of Physics and Astronomy, University of Aarhus, Ny Munkegade, Building 520, DK-8000 Aarhus C, Denmark; Electronic address: jvanelp@dfi.aau.dk
- <sup>1</sup>B. T. Thole, G. van der Laan, and G. A. Sawatzky, *Phys. Rev. Lett.* **55**, 2086 (1985).
  - <sup>2</sup>G. van der Laan, B. T. Thole, G. A. Sawatzky, J. B. Goedkoop, J. C. Fuggle, J.-M. Esteve, R. Karnatak, J. P. Remeike, and H. A. Dabkowska, *Phys. Rev. B* **34**, 6529 (1986).
  - <sup>3</sup>G. Schütz, W. Wagner, W. Wilhelm, L. Kienle, R. Zeller, R. Frahm, and G. Materlik, *Phys. Rev. Lett.* **58**, 737 (1987).
  - <sup>4</sup>P. Rudolf, F. Sette, L. H. Tjeng, G. Meigs, and C. T. Chen, *J. Magn. Magn. Mater.* **109**, 288 (1992).
  - <sup>5</sup>R. Wienke, G. Schütz, and H. Ebert, *J. Appl. Phys.* **69**, 6147 (1991).
  - <sup>6</sup>T. Böske, W. Clemens, C. Carbone, and W. Eberhardt, *Phys. Rev. B* **49**, 4003 (1994).
  - <sup>7</sup>B. T. Thole, P. Carra, F. Sette, and G. van der Laan, *Phys. Rev. Lett.* **68**, 1943 (1992).
  - <sup>8</sup>P. Carra, B. T. Thole, M. Alterelli, and X. Wang, *Phys. Rev. Lett.* **70**, 694 (1993).
  - <sup>9</sup>J. van Elp, S. J. George, J. Chen, G. Peng, C. T. Chen, L. H. Tjeng, G. Meigs, H.-J. Lin, Z. H. Zhou, M. W. W. Adams, B. G. Searle, and S. P. Cramer, *Proc. Natl. Acad. Sci. U.S.A.* **90**, 9664 (1993).
  - <sup>10</sup>G. Palmer, W. R. Dunham, J. A. Fee, R. H. Sands, T. Iizuka, and T. Yonetani, *Biochem. Biophys. Acta* **245**, 201 (1971).
  - <sup>11</sup>L. Petersson, R. Cammack, and K. R. Rao, *Biochim. Biophys. Acta* **622**, 18 (1980).
  - <sup>12</sup>C. T. Chen and F. Sette, *Rev. Sci. Instrum.* **60**, 1616 (1989).
  - <sup>13</sup>S. P. Cramer, J. Chen, S. J. George, J. van Elp, J. Moore, O. Tensch, J. Colaresi, M. Yocum, O. C. Mullins, and C. T. Chen, *Nucl. Instrum. Methods Phys. Res. Sect. A* **319**, 285 (1992).
  - <sup>14</sup>R. H. Sands and W. R. Dunham, *Q. Rev. Biophys.* **7**, 443 (1975).
  - <sup>15</sup>J. Cárdenas, L. E. Mortenson, and D. C. Yoch, *Biochim. Biophys. Acta* **434**, 244 (1975).
  - <sup>16</sup>L.-C. Duda, J. Stöhr, D. C. Mancini, A. Nilsson, N. Wassdahl, J. Nordgren, and M. G. Samant, *Phys. Rev. B* **50**, 16 758 (1994).
  - <sup>17</sup>S. J. George, J. van Elp, J. Chen, Y. Ma, C. T. Chen, J.-B. Park, M. W. W. Adams, B. G. Searle, F. M. F. de Groot, J. C. Fuggle, and S. P. Cramer, *J. Am. Chem. Soc.* **114**, 4426 (1992).
  - <sup>18</sup>G. van der Laan and I. W. Kirkwood, *J. Phys. Condens. Matter* **4**, 4189 (1992).
  - <sup>19</sup>G. van der Laan, B. T. Thole, G. A. Sawatzky, and M. Verdaguer, *Phys. Rev. B* **37**, 6587 (1988).
  - <sup>20</sup>F. M. F. de Groot, J. C. Fuggle, B. T. Thole, and G. A. Sawatzky, *Phys. Rev. B* **41**, 928 (1990).
  - <sup>21</sup>J. van Elp, G. Peng, B. G. Searle, S. Mitra-Kirtley, Y.-H. Huang, M. K. Johnson, Z. H. Zhou, M. W. W. Adams, M. J. Maroney, and S. P. Cramer, *J. Am. Chem. Soc.* **116**, 1918 (1994).
  - <sup>22</sup>The spectra are calculated in a  $T_d$  symmetry and are broadened at the  $L_3$  ( $L_2$ ) edge with a Lorentzian of 0.25 (0.5) eV for the  $d^5$  ( $\text{Fe}^{3+}$ ) initial state and 0.2 (0.4) eV for the  $d^6$  ( $\text{Fe}^{2+}$ ) initial state, and convoluted with a Gaussian of 0.25 eV.
  - <sup>23</sup>E. U. Condon and G. H. Shortley, *The Theory of Atomic Spectra* (Cambridge University Press, Cambridge, England, 1959).
  - <sup>24</sup>J. Peisach, W. E. Blumberg, E. T. Lode, and M. J. Coon, *J. Biol. Chem.* **246**, 5877 (1971).
  - <sup>25</sup>M. S. Gebhard, J. C. Deaton, S. A. Koch, M. Millar, and E. I. Solomon, *J. Am. Chem. Soc.* **112**, 2217 (1990).
  - <sup>26</sup>M. S. Gebhard, S. A. Koch, M. Millar, F. J. Devlin, P. J. Stephens, and E. I. Solomon, *J. Am. Chem. Soc.* **113**, 1640 (1991).
  - <sup>27</sup>J. van Elp, S. J. George, G. Peng, B. G. Searle, Z. H. Zhou, M. W. W. Adams, and S. P. Cramer, *Proc. SPIE* **2010**, 181 (1994).
  - <sup>28</sup>W. R. Dunham, A. J. Bearden, I. T. Salmeen, G. Palmer, R. H. Sands, W. H. Orme-Johnson, and H. Beinert, *Biochem. Biophys. Acta* **523**, 134 (1971).